# Preparation and Application of Copper Oxide Nanoparticles

M. H. Chang and Clifford Y. Tai*

*Department of Chemical Engineering, National Taiwan University
Taipei, Taiwan, cytai@ntu.edu.tw

## ABSTRACT

Copper oxide nanoparticles were synthesized in this study using a spinning disk reactor (SDR). The precursor of copper oxide was first synthesized by a liquid-liquid reaction of $CuSO_4$ and $Na_2CO_3$ solutions in a continuous mode using SDR. Then the precursor was calcined up to 500°C to obtain copper oxide nanoparticles. The effects of operating variables, including rotation speed, reactant concentration, and liquid flow rate, on the size of copper oxide nanoparticles were investigated. Smaller copper oxide particles were obtained under lower reactant concentration and higher disk rotation speed. The size of obtained primary particles of copper oxide was between 20-30 nm observed under a transmission electron microscope as compared to the number mean size of 40-50 nm determined by a particle size analyzer. Then a CuO-water nanofluid was prepared and the effective thermal conductivity of the CuO-water nanofluid increased with an increase in CuO content up to 0.40 vol%.

***Keywords***: spinning disk reactor, nanofluid, copper oxide, nanoparticle

## 1 INTRODUCTION

Nanofluid is a system that is composed of nanoparticles dispersed in a heat transfer fluid in order to enhance the thermal conductivity, specific heat capacity, and electrical conductivity of the fluid. One of the methods reported in the literature, for synthesizing nanofluid was called VEROS (vacuum evaporation on running oil substrate) [1]. Magnetic materials such as iron, cobalt, and nickel were straightly evaporized into silicon oil to obtain nanofluid, in which the size of nanoparticles was about 2.5 nm. A similar method using evaporation/condensation technique, called SANSS (submerged arc nanoparticle synthesis system), was reported by Jwo et al. [2] to prepare CuO-water nanofluid using a high temperature arc between 6000-12000 °C, and the thermal conductivity of the nanofluid can be improved by 9.6 % as the CuO content of 0.4 vol%. Lee et al. [3] has prepared $Al_2O_3$ and CuO nanoparticles using the condensation method and then dispersed them in a mixing chamber to obtain nanofluid. The thermal conductivities of CuO-water nanofluid were were improved by 12 % as the CuO content of 3.4 vol%. Although the thermal conductivity of the fluid can be increased by these methods, the production rate need to be improved and aggregation of particles need to be solved. Furthermore, these processes were time and energy consuming, and the manufacturing processes were difficult to scale-up.

One possible method for mass production of nanoparticles is the HiGee technique, which has been developing for more than ten years. Two types of equipments, i.e., rotating packed-bed reactor (RPBR) and spinning disk reactor (SDR), have been applied in this regard [4-6]. For using the SDR in crystallization, reactant solutions were spread onto a spinning disk to achieve a uniform and high supersaturation through micromixing, thus small and uniform particles were obtained via precipitation. In our laboratory, uniform nanoparticles of different chemicals, such as barium carbonate [7], magnesium hydroxide [8], and silver nanoparticles [9,10], has been successfully synthesized using this technique, and the production rate was greatly improved, i.e., 33 kg/day for silver nanoparticles.

In this research, copper oxide particles were synthesized by using an SDR, with the expectation of a product of the uniform and nano-scale particles, and the effects of operating variables were also investigated. The produced copper oxide particles were further used to prepare nanofluid, and the thermal conductivity was measured using the transition hot-wire method.

## 2 EXPERIMENTAL

### 2.1 Preparation of the Precursor and CuO Nanoparticles

The experimental setup of continuous operating is shown in Fig. 1. It consists of a liquid feeding system (1~8), a spinning disk reactor (9 and 10), a slurry outlet (11) and a collection tank (12). The liquid feeding system contains two storage tanks (1 and 2), from which liquid reactants are pumped into the reactor chamber through flowmeters (5 and 6). Two liquid distributors (7 and 8) perpendicular to the spinning disk (9) were designed to distribute the reactants uniformly on the disk. The main part of the spinning disk reactor is a stainless-steel disk (9), which is 20 cm in diameter and driven by a variable-speed motor (M). The spinning disk is enclosed in a cylindrical acrylic-chamber (10). A funnel-like outlet (11) is located at the bottom of the chamber for guiding the slurry into the collection vessel (12).

At the beginning of an experiment, one-liter $CuSO_4 \cdot 5H_2O$ and $Na_2CO_3$ solutions with concentrations ranging

from 0.01 M to 0.40 M were charged separately into tanks 1 and 2. The two reactant solutions were pumped onto the center of the spinning disk at a rotation speed N through the two distributors at a controlled flow rate ($L_1$, $L_2$). Then the liquid velocity was accelerated due to centrifugal force, causing it to spread over the disk surface and forming a thin film where the precursor of copper oxide precipitated. The slurry left the disk, hit the inner wall of the chamber, flowed down along the wall past the funnel-like outlet, and was finally collected in the vessel. The product slurry was centrifuged at 11,000 rpm for 10 minutes, washed with deionized water and acetone, and finally dried in vacuum for one day at room temperature. Then the produced precursor powder was subjected to a calcination process up to 500$^{o}$C to produce CuO powder.

## 2.2 Characterization of the Precursor and CuO nanoparticles

Powder samples were then analyzed with an X-ray diffractometer (XRD, Philips, X'PERT) to determine their crystal structures, and their morphologies were observed with a transmission electron microscope (JEOL, JEM1010). To determine the particle size distribution, CuO powder was dispersed in water agitated with a sonicator (Misonix, XL2020), using sodium hexametaphosphate (Kokusan Chemical Works, Ltd.) as dispersant, and was analyzed with a dynamic light scattering analyzer (Malvern, nano ZS). The functional groups of the precursor of copper oxide were also determined by using a Fourier transform infrared spectroscope (FT-IR, BIO-RAD FTS3000). The weight change of the precursor during the calcination process was analyzed by a thermalgravimetric analyzer (TGA, PerkinElmer Pyris 1 TGA) under nitrogen environment.

## 2.3 Preparation of CuO Nanofluid and The Measurement of Thermal Conductivity

To prepare CuO-water nanofluid, NaHMP was used as the dispersant with the concentration ranging from 0.2 to 2 g/100mL. The produced CuO powder of desired amount was agitated for 10 min in a jacketed vessel containing NaHMP solution kept at room temperature using sonicator with a power intensity of 165 W. Effective thermal conductivity of nanofluid was measured by a Thermal Properties Analyzer (Decagon, KD2), which consists of a handheld readout and a 6 cm stainless needle sensor that can be inserted into the fluid. The measurement theory was based on transient hot-wire method [3].

# 3 RESULTS AND DISCUSSION

For synthesizing copper oxide, the effects of operating variables were investigated, including reactant concentration, reactant flow rate, and rotation speed of SDR. Characteristics of the precursor and copper oxide were also determined. The produced copper oxide nanoparticles were further used for preparing nanofluid, and the thermal conductivity was measured and compared with that calculated by theoretical model.

## 3.1 Effects of Reactant Concentration on the CuO particle size

In order to investigate the effects of the reactant concentration on the CuO particle size, other operating variables were fixed: the liquid flow rates of $CuSO_4 \cdot 5H_2O$ and $Na_2CO_3$ solution set at 0.2 L/min, the rotation speed of the spinning disk at 4000rpm, and the $[CuSO_4 \cdot 5H_2O]/[Na_2CO_3]$ ratio at 1/1 according to the stoichiometric ratio of the reaction. The results were shown in Table 1. When the concentration of copper sulfate, $[CuSO_4 \cdot 5H_2O]$, was smaller than 0.10 M, the change in particle size was less significant. Then the mean size of particles increased dramatically with increasing reactant concentrations. As the concentration of copper sulfate increased from 0.10 M to 0.40 M, the volume mean size of CuO increased nearly threefold, from 63.3 to 167.2 nm, and the number mean size was almost doubled, from 48.3 nm to 93.0 nm. The reason was conjectured as follows: under all the controlled reactant concentrations, the nucleation took place were at an extremely fast rate, and resulted in uniform, tiny primary particles. However, under higher concentrations, the tiny nuclei collided with each other more easily to yield more agglomerates.

## 3.2 Effects of Reactant Flow Rate on the CuO Particle size

In this experiment, the concentration of $CuSO_4 \cdot 5H_2O$ and $Na_2CO_3$ solution fixed at 0.1 M, and the rotation speed at 4000 rpm, the liquid flow rates of both reactant solutions were changed simultaneously from 0.2 L/min to 5.0 L/min to see how they affect the CuO particle size. The results indicated that when the liquid flow rate was increased from 0.2 L/min to 3.0 L/min, both the volume and number mean size of copper oxide changed very little, with a variation within 4 nm from the average, which was 61.3 nm and 47.0 nm respectively. For a further increase in the flow rate to 5.0 L/min, the volume mean size of CuO particles jumped from 59.2 to 74.6 nm and the number mean size increased from 44.5 to 51.5 nm. It was understood that an increase in liquid flow rate resulted in a thicker liquid film on the spinning disk, and thus, a worse mixing between the two reactant solutions. The poor mixing caused an incomplete reaction on the disk surface. As a result, the residual reactants further reacted in the collection vessel, where the crystals grew to form larger particles with a wider distribution.

### 3.3 Effects of Rotation Speed on the CuO Particle Size

As to the effect of rotation speed of the disk was concerned, the mean sizes of CuO particles obtained under different rotation speeds of the disk were measured, and the flow rates of both reactant solutions were kept at 1.5 L/min. When the rotation speed increased from 1000 rpm to 4000 rpm, the volume and number mean size of copper oxide remained almost constant, about 60 and 46 nm, respectively. As the disk rotation speed was below 1000 rpm, i.e., at 500 rpm, the volume mean size of CuO increased to 79.3 nm. Lower rotation speed of the disk caused poorer agitation and less disturbances within the liquid film, and thus, the lower mixing efficiency. As a result, the particle size distribution of CuO product was wider, just like the case of high flow rate of reactants.

### 3.4 Analysis of the Precursor and CuO particles

To determine the chemistry of calcination process leading the decomposition of precursors to form copper oxide, the precursors were subject to FT-IR and TGA analyses. The FT-IR pattern of the produced precursor of CuO was shown in Fig. 2. Both OH and $CO_3$ bondings were observed, predicting the precursor to be $Cu_2(OH)_2CO_3$ compound. As to the TGA analysis, the precursor sample was heated to 600 °C with a heating rate of 10 °C/min, and the final weight percentage remained almost constant at temperatures above 500 °C was 74.5 %, which was closed to the theoretical molecular weight ratio, 2CuO/ $Cu_2(OH)_2CO_3$, of 72 % predicted by the following equation (1). This small difference could be attributed to some impurity which was included in the precursor.

$$Cu_2(OH)_2CO_{3(s)} \xrightarrow{\Delta} 2CuO_{(s)} + CO_2 \uparrow + H_2O \qquad (1)$$

Figure 3(a) shows the results of XRD analysis of the CuO product, which indicates a tenorite structure. The TEM micrograph shown in Fig. 3(b) revealed that the morphology of CuO was spherical, 20-30 nm in diameter, with some aggregates of 50-100 nm. The mean particle size measured by a dynamic light scattering analyzer was 40-50 nm and 60-70 nm for number and volume, respectively. The particle size distribution is shown in Fig. 4, and the percentage of CuO particle smaller than 100 nm is greater than 90 vol%.

### 3.5 Thermal Conductivity of CuO Nanofluid

The effective thermal conductivities under CuO content ranging from 0.01 to 0.40 vol% were measured and compared with that by theoretical calculation using Maxwell model [11]. The thermal conductivity of the nanofluid was increased as the CuO content increased, and the best result of this research was more than 10% improvement as CuO content was 0.40 vol%. In addition, the thermal conductivity of all the samples of nanofluid were higher than that of calculated, which was 1.01 as CuO content of 0.40 vol%. It was probably due to the simplicity of the model which neglected the effects of motion, interaction, and size of particles.

## 4 CONCLUSION

Copper oxide nanoparticles were successfully synthesized using the spinning disk reactor. The effects of operating variables on particle size were investigated. Smaller copper oxide particles were obtained under lower reactant concentration and higher disk rotation speed. Spherical copper oxide nanoparticles with size 20-30 nm were observed under an electron microscope, and their volume mean size was about 60-70nm measured by a dynamic light scattering analyzer. For the prepared CuO nanofluid, the thermal conductivities of all the samples were higher than that calculated from theoretical model, showing that CuO nanoparticles has great potential for the heat transfer application.

## 5 TABLES AND ILLUSTRATIONS

| $[CuSO_4 \cdot 5H_2O]$ (M) | volume mean size (nm) | number mean size (nm) |
|---|---|---|
| 0.01 | 56.7 | 44.2 |
| 0.05 | 60.3 | 45.7 |
| 0.10 | 63.3 | 48.3 |
| 0.20 | 94.3 | 63.7 |
| 0.30 | 122.3 | 75.3 |
| 0.40 | 167.2 | 93.2 |

Table 1: Effect of reactant concentration on CuO particle size. Other operating conditions: $L_1=L_2=0.2$ L/min, N= 4000rpm, $[CuSO_4 \cdot 5H_2O]/ [Na_2CO_3]= 1$

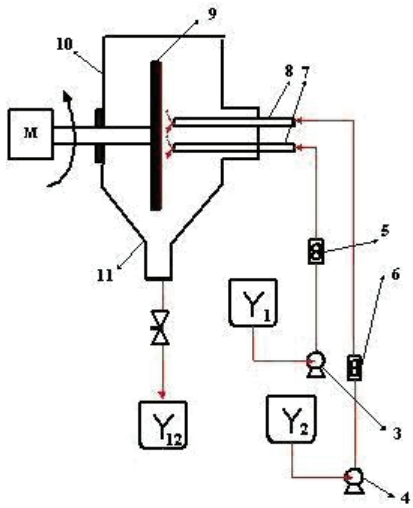


1,2: storage tank 3,4: pump 5,6: flowmeter
7,8: liquid distributor 9: spinning disk 10: chamber
11: outlet 12: collection tank M: motor

Figure 1 Experimental Setup.

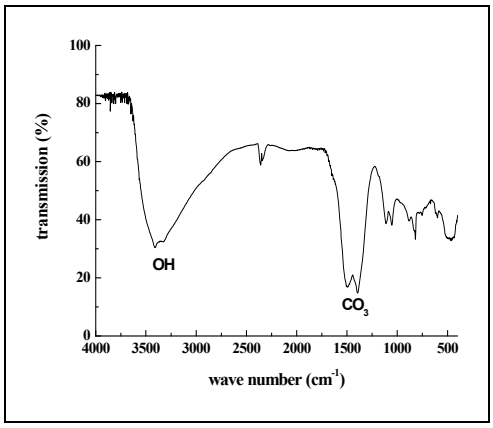


Figure 2 FT-IR pattern of the precursor of copper oxide.

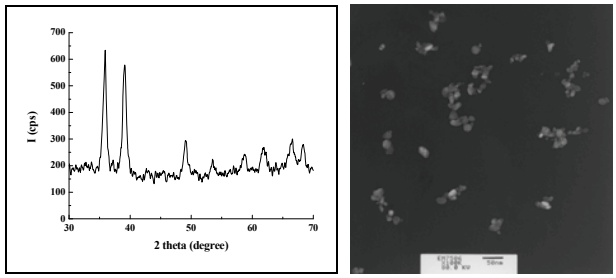


Figure 3 (a)XRD pattern; (b) TEM micrograph of produced CuO nanoparticles.

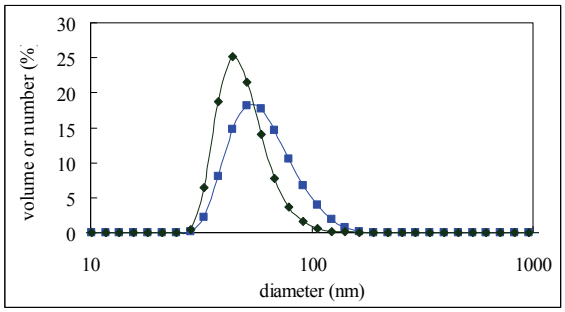


Figure 4 CuO particle size distribution on volume basis (■) and number basis (◆).

## ACKNOWLEDGMENTS

The authors wish to thank the National Science Council of Taiwan for financial support of this work.

## REFERENCES

[1] H. Akoh, Y. Tsukasaki, S. Yatsuya, and A. Tasaki, J. Cryst. Growth 45, 495, 1978.
[2] C. S. Jwo, T. P. Teng, and J. Chang, J. Alloy. Compd. 434-435, 569, 2007.
[3] S. Lee, S. U. S. Choi, S. Li, and J. A. Eastman, Trans. Am. Soc. Mech. Eng. 121, 280, 1999.
[4] C. Ramshaw and R. H. Mallinson, US Patent 4383255, 1981.
[5] J. F. Chen, Y. H. Wang, F. Guo, X. M. Wang, and C. Zheng, Ind. Eng. Chem. Res. 39, 948, 2000.
[6] L. M. Cafiero, G. Baffi, A. Chianese, and R. J. J. Jachuck, Ind. Eng. Chem. Res. 41, 5240, 2002.
[7] C. Y. Tai, C. T. Tai, and H. S. Liu, Chem. Eng. Sci. 61, 7479, 2006.
[8] C. Y. Tai, C. T. Tai, M. H. Chang, and H. S. Liu, Ind. Eng. Chem. Res. 46, 5536, 2007.
[9] C. Y. Tai, Y. H. Wang, and H. S. Liu, AIChE J. 54, 445, 2008.
[10] C. Y. Tai, Y. H. Wang, C. T. Tai, and H. S. Liu, Ind. Eng. Chem. Res. 48, 10104, 2009.
[11] J. C. Maxwell, "A Treatise on Electricity and Magnetism," Vol. 1, Clarendon Press: Oxford, 1881.